Circulation Journal
Circ J 2023; 87: 329–335
doi:10.1253/circj.CJ-22-0299

ORIGINAL ARTICLE
Imaging

Association of Microluminal Structures Assessed by Optical Coherence Tomography With Local Inflammation in Adjacent Epicardial Adipose Tissue and Coronary Plaque Characteristics in Fresh Cadavers

Yutaka Kawabata, MD, PhD; Tetsuzo Wakatsuki, MD, PhD, FJCS; Koji Yamaguchi, MD, PhD; Daiju Fukuda, MD, PhD; Hiroyuki Ito, MD, PhD; Tomomi Matsuura, MD, PhD; Kenya Kusunose, MD, PhD, FJCS; Takayuki Ise, MD, PhD; Shusuke Yagi, MD, PhD; Hirotsugu Yamada, MD, PhD, FJCS; Takeshi Soeki, MD, PhD, FJCS; Yoshihiro Tsuruo, MD, PhD; Masataka Sata, MD, PhD, FJCS

Background: Coronary intraplaque microluminal structures (MS) are associated with plaque vulnerability, and the inward progression of vascular inflammation from the adventitia towards the media and intima has also been demonstrated. Therefore, in the present study we investigated the relationships among MS, local inflammation in adjacent epicardial adipose tissue (EAT), and coronary plaque characteristics.

Methods and Results: Optical coherence tomography (OCT) revealed MS in the left anterior descending coronary artery in 10 fresh cadaveric hearts. We sampled 30 lesions and subdivided them based on the presence of MS: MS (+) group (n=19) and MS (–) group (n=11). We measured inflammatory molecule levels in the adjacent EAT and percentage lipid volume assessed by integrated backscatter intravascular ultrasound in each lesion. The expression levels of vascular endothelial growth factor B and C-C motif chemokine ligand 2 were significantly higher in the MS (+) group than in the MS (–) group (0.9±0.7 vs. 0.2±0.2 arbitrary units (AU), P=0.04 and 1.5±0.5 vs. 0.6±0.7 AU, P=0.02, respectively). Percentage lipid volume was significantly higher in the MS (+) group than in the MS (–) group (38.7±16.5 vs. 23.7±10.9%, P=0.03).

Conclusions: Intraplaque MS observed on OCT were associated with lipid-rich plaques and local inflammation in the adjacent EAT. Collectively, these results suggest that local inflammation in the EAT is associated with coronary plaque vulnerability via MS.

Key Words: Coronary plaque; Inflammatory molecules; Microluminal structures; Optical coherence tomography

The inward progression of vascular inflammation from the adventitia towards the media and intima has been reported,[1–4] and the growth of atherosclerotic plaque is accompanied by neovascularization from the vasa vasorum (VV).[5–8] Adipocytokines secreted from perivascular adipose tissue have direct access to the adjacent arterial wall via diffusion or the VV.[9,10] We reported that human coronary atherosclerosis is associated with inflammatory responses in epicardial adipose tissue (EAT) and also that the infiltration of macrophages and expression of pro- and anti-inflammatory cytokines in EAT are higher in patients with than in those without coronary artery disease (CAD).[11]

Coronary intraplaque microluminal structures (MS) are associated with plaque vulnerability and progression.[12,13] Although optical coherence tomography (OCT) enables the detection of MS through high-resolution imaging technology,[14,15] understanding of the relationships among local EAT, coronary intraplaque MS, and coronary plaque formation in humans is limited.

In the present study we investigated the relationships among intraplaque MS detected by OCT, coronary plaque characteristics assessed by integrated backscatter intravascular ultrasound (IB-IVUS), and inflammatory molecule

Received May 19, 2022; revised manuscript received August 30, 2022; accepted September 10, 2022; J-STAGE Advance Publication released online October 15, 2022 Time for primary review: 19 days
Department of Cardiovascular Medicine (Y.K., T.W., K.Y., T.M., K.K., T.I., S.Y., T.S., M.S.), Department of Community Medicine for Cardiology (H.I., H.Y.), Department of Community Medicine and Medical Science (T.S.), Department of Anatomy (Y.T.), Tokushima University Graduate School of Biomedical Sciences, Tokushima; Department of Cardiovascular Medicine, Osaka Metropolitan University Hospital, Osaka (D.F.), Japan
Mailing address: Tetsuzo Wakatsuki, MD, PhD, FJCS, Department of Cardiovascular Medicine, Tokushima University Graduate School of Biomedical Sciences, 3-18-15 Kuramoto-cho, Tokushima 770-8503, Japan. email: wakatsukitz@tokushima-u.ac.jp

ISSN-1346-9843

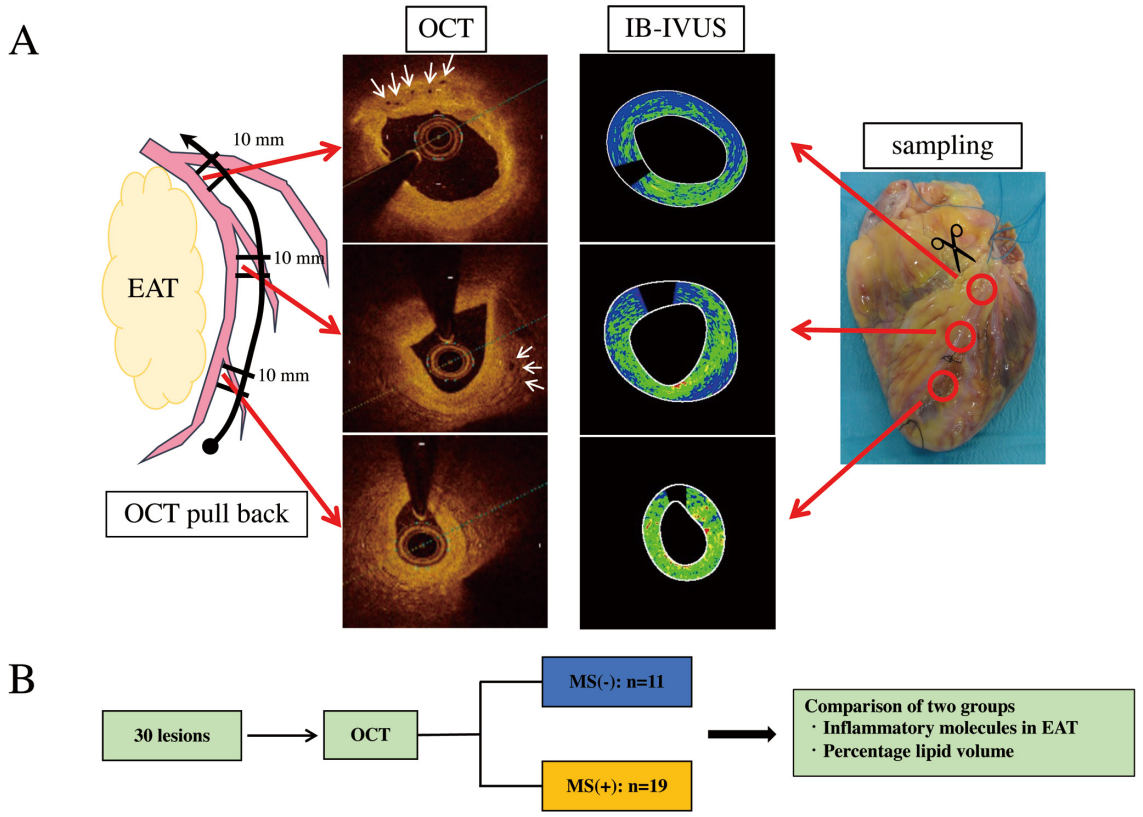

Figure 1. (**A**) Study design and representative OCT and IB-IVUS images of coronary artery plaques. MS are indicated by white arrows. Inflammatory molecules were measured in adjacent epicardial adipose tissue (EAT). (**B**) The 30 lesions were divided the MS (+) and MS (−) groups. IB-IVUS, integrated backscatter intravascular ultrasound; MS, microluminal structures; OCT, optical coherence tomography.

measurements in the adjacent EAT in fresh cadaveric hearts.

Methods

Cadavers and Study Design

Fresh cadavers (n=10) stored at −20°C were returned to a natural, fresh cadaveric state by thawing fresh-frozen cadavers for ≥24 h. The hearts were removed and cleaned with normal saline. A 0.014-inch guidewire was introduced into the left anterior descending coronary artery (LAD) for evaluation with a frequency-domain OCT system (OPTIS™ Mobile System; Abbott, Santa Clara, CA, USA). The LAD was divided into 3 equal parts distal to proximal and lesions with prominent MS in each of the parts were sampled; lesions without MS were sampled as controls. All sampling points were limited to sites with ≥25% plaque burden evaluated on IB-IVUS. Lesions were classified into 2 groups based on the number of MS identified by OCT: MS (+) group (≥1 MS) and MS (−) group. We also measured local inflammatory molecule levels in the adjacent EAT and assessed percentage lipid volume by IB-IVUS in each lesion (**Figure 1**). In the cadaveric hearts, the OCT probe light could be seen on the surface. The OCT pullback system was used manually, so the site to be observed was accurately identified, enabling precise sampling of adjacent EAT. Furthermore, the distance from the coronary orifice or a characteristic side branch to the point to be examined was measured, and IVUS was performed at the site that was consistent with the distance measured on IVUS. The study protocol was approved by the Institutional Review Board of Tokushima University Hospital.

OCT Data Acquisition

Following the passage of the guidewire into the LAD, the 2.7-Fr OCT imaging catheter (Dragonfly™ OPTIS™ Imaging Catheter, Abbott) was introduced over the wire and positioned as distal as possible to the LAD, and automated pullback at 18 mm/s was then performed. If necessary, the position of the probe was manually established and detailed observations/recordings were conducted. While performing OCT, the intracoronary space was filled with physiological saline and pullback was conducted while manually and continuously adding a sufficient perfusion pressure to maintain the MS shape and obtain favorable images. In the segmental analysis, the length of each segment was defined as 10 mm, and each segment was separated from the adjacent segment by at least 20 mm. MS was defined as a no-signal tubuloluminal structure with a diameter of 50–150 μm and no connection to the vessel lumen that was observed in ≥3 consecutive cross-sectional OCT images.[15] The total number of MS was

identified. OCT measurements were performed by 2 independent physicians who were blinded to the clinical data for the cadavers.

IVUS Data Acquisition and IB-IVUS Parameters

Following the passage of the guidewire into the LAD, after OCT, the IVUS catheter (40 MHz; ViewIT, Terumo) was introduced over the wire and each lesion assessed by OCT was observed. Saline was infused into the LAD with a constant manual perfusion pressure to obtain clear images. Data were collected at an auto pullback rate of 0.5 mm/s and analyzed using IVUS imaging system (VISIWAVE, Terumo). For each lesion, 10 IB-IVUS images (10 mm in length) were captured at 1-mm intervals using a motorized pullback system. The cross-sectional lumen area, cross-sectional vessel area within the external elastic membrane, and plaque area (the external elastic membrane area minus the lumen area) were calculated using software attached to the IVUS system. Regarding plaque assessment, IVUS appears be more useful than OCT because the entire plaque can be quantitatively evaluated. We have reported plaque properties using IB-IVUS,[16–18] so we also used it for plaque assessments in this study. The IB values for each histological category were defined by comparisons with histological images from a previous study.[19] Plaque properties were classified into 4 types based on a combination of the spectral parameters of the posterior scattering signals of IVUS: lipid pool, fibrosis, dense fibrosis, or calcification. Percentage lipid volume was calculated using integration. IB-IVUS measurements were performed by 2 independent physicians who were blinded to the clinical data for the cadavers.

Inflammatory Molecule Measurements

After performing OCT, the vessels and adjacent EAT of each lesion were trimmed from the LAD for measurement of the expression levels of inflammatory molecules (vascular endothelial growth factor A [VEGFA], VEGFB, VEGFC, C-C motif chemokine ligand 2 [CCL2], adiponectin [ADIPOQ], and glycerol-3-phosphate dehydrogenase [G3PDH]) were measured in each sample of EAT. Total RNA was extracted using the Illustra RNAspin RNA Isolation Kit (GE Healthcare). cDNA was synthesized from 100 ng of total RNA extracted from tissues and cells using the QuantiTect Reverse Transcription Kit (Qiagen). A real-time quantitative polymerase chain reaction (qPCR) was performed using Mx3000P (Agilent Technologies) and Power SYBR Green PCR Master Mix (Applied Biosystems). The primer sequences used were as follows: *VEGFA*, 5'-AAGGAGGAGGGCAGAATCAT-3' (sense) and 5'-ATCTGCATGGTGATG TTGGA-3' (antisense); *VEGFB*, 5'-GGCTTAGAGCTCAACCCAGA-3' (sense) and 5'-GAC AAGGGATGGCAGAAGAG-3' (antisense); *VEGFC*, 5'-AAAGAACCTGCCCCAGAAAT-3' (sense) and 5'-GAAAATCCTGGCTCACAAGC-3' (antisense); *CCL2*, 5'-CCCCAGTCACCT GCGTTAT-3' (sense) and 5'-AGATCTCCTTGGCCACAATG-3' (antisense); *ADIPOQ*, 5'-GTGATGGCAGAGATGGCAC-3' (sense)

Table 1. Baseline Characteristics of the Cadavers

Cadaver no.	Age, sex	Cause of death*
1	70, F	Muscular dystrophy
2	80, F	Caducity
3	96, F	Pneumonia
4	70, M	Amyloidosis
5	77, M	Respiratory failure
6	95, F	Caducity
7	69, F	Multiple organ failure
8	74, F	Brain cancer
9	93, M	Chronic obstructive pulmonary disease
10	87, F	Caducity

*From death certificate.

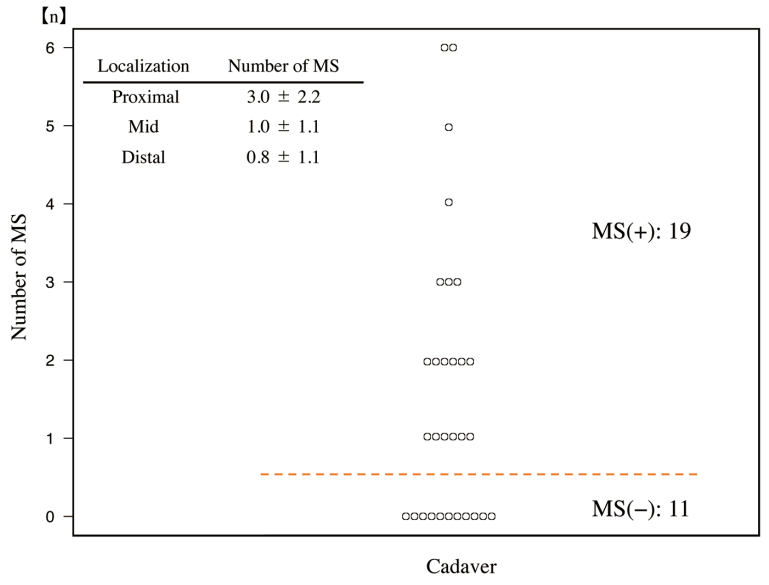

Figure 2. Classification according to the number and localization of microluminal structures (MS) identified by optical coherence tomography.

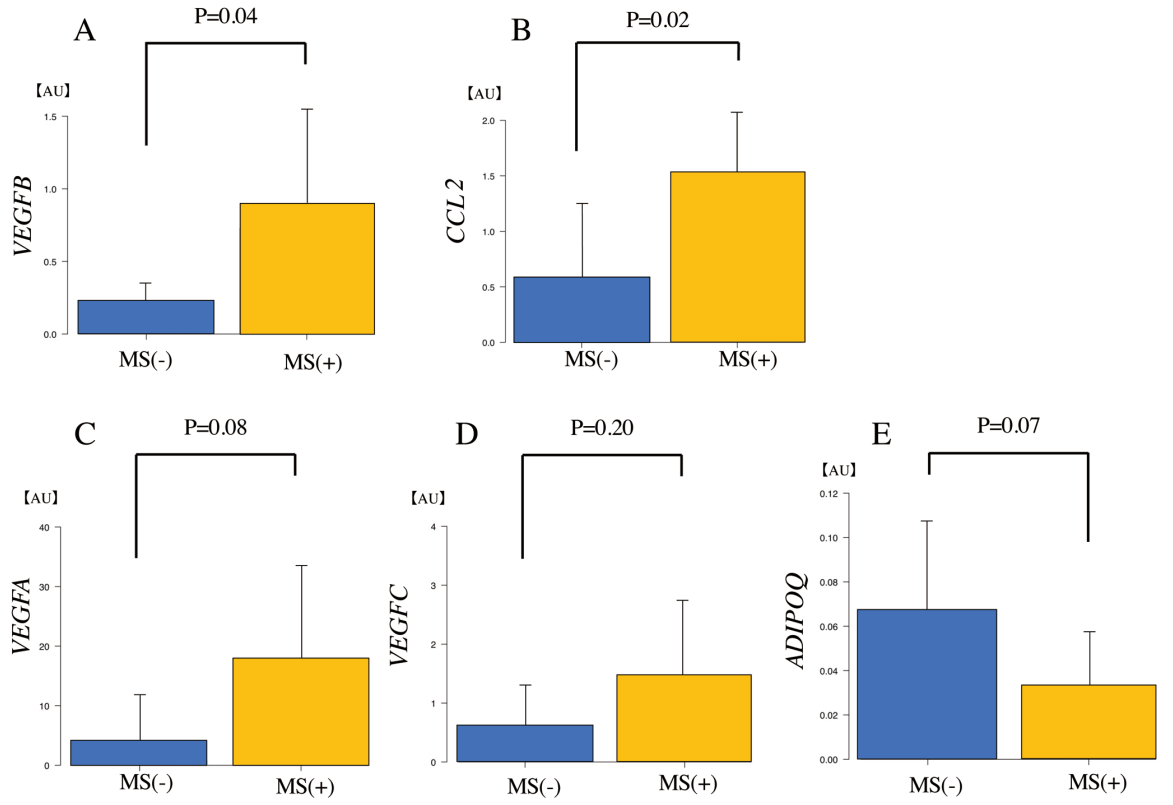

Figure 3. (**A**–**E**) Comparison of the expression of inflammatory molecules in adjacent epicardial adipose tissue between the groups with presence [MS (+)] and absence [MS (−)] of microluminal structures. *ADIPOQ*, adipocyte-specific protein; *CCL2*, C-C motif chemokine ligand 2; *VEGFA*, *-B*, *-C*, vascular endothelial growth factor A, B, C.

and 5'-ACACTGAATGCTGAGCGGTA-3' (antisense); and *G3PDH*, 5'-TGGGTGTGAACCATGAGAAG-3' (sense) and 5'-GCTAAGCAGTTGGTGGTGC-3' (antisense). Expression levels were normalized against that of *G3PDH* and quantified in arbitrary units (AU).

Statistical Analysis

All data are expressed as the mean±SD. An unpaired Student's t-test was used to test the significance of differences in each parameter between the MS (+) and MS (−) groups. Significance was indicated by $P<0.05$. All statistical analyses were performed using EZR (Saitama Medical Center, Jichi Medical University, Saitama, Japan), which is a graphical user interface for R (The R Foundation for Statistical Computing, Vienna, Austria). Specifically, it is a modified version of the R commander that was designed to add statistical functions that are frequently used in biostatistics.[20]

Results

Cadaveric Characteristics

The characteristics of the 10 fresh-frozen cadavers are summarized in **Table 1**. The mean age was 81.1 years (range, 69–96 years) and only the following characteristics were identified: age, sex, and cause of death; none had died of cardiovascular disease.

Lesion Classification

The 30 lesions were divided into the MS (+) group (n=19) and MS (−) group (n=11) (**Figure 2**) based on the number of MS identified by OCT. The number of MS was higher in proximal lesions than in other lesions (**Figure 2**).

Inflammatory Molecule Expressions

The expression levels of *VEGFB* and *CCL2* in the adjacent EAT were higher in the MS (+) group than in the MS (−) group (0.9±0.7 vs. 0.2±0.2 AU, P=0.04 and 1.5±0.5 vs. 0.6±0.7 AU, P=0.02, respectively). No significant differences were observed in the expression levels of *VEGFA*, *VEGFC*, or *ADIPOQ* between groups (**Figure 3**).

IB-IVUS Measurements

Conventional IVUS and IB-IVUS parameters are shown in **Table 2**. Percentage dense fibrous volume was significantly higher in the MS (−) group than in the MS (+) group (15.2±9.3 vs. 7.7±4.2%, P=0.04), whereas percentage lipid volume was significantly higher in the MS (+) group than in the MS (−) group (38.7±16.5 vs. 23.7±10.9%, P=0.03) (**Figure 4**).

Discussion

Recent studies suggest that adipokines and inflammatory molecules secreted from EAT significantly affect the myo-

Table 2. Conventional IVUS and IB-IVUS Parameters

	MS (+) group (n=19)	MS (–) group (n=11)	P value
Mean vessel area (mm^2)	8.6±2.6	7.2±4.1	0.3
Mean lumen area (mm^2)	4.0±1.1	3.5±1.7	0.4
Plaque volume (mm^3)	20.3±6.7	16.1±10.4	0.2
Fibrous volume (%)	52.0±12.2	58.7±4.8	0.1
Lipid volume (%)	38.7±16.5	23.7±10.9	0.03
Dense fibrous volume (%)	7.7±4.2	15.2±9.3	0.04
Calcified volume (%)	1.5±1.3	2.5±2.2	0.3

IB-IVUS, integrated backscatter intravascular ultrasound; MS, microluminal structure.

cardium and coronary arteries.[21] The quality of EAT, including its inflammatory status, has been shown to affect cardiac and coronary vascular functions.[22] Several adipokines and inflammatory molecules secreted from EAT diffuse through the interstitial fluid across the adventitia, media, and intima and may interact with the VV, endothelial cells, and vascular smooth muscle cells of the coronary vasculature, which may in turn result in inflammation, endothelial and smooth muscle cell proliferation, atherogenesis, and atherosclerotic plaque destabilization.[9,10] However, limited information is currently available on the relationship between local inflammation in EAT and MS growth in coronary plaques in vivo. Our results from cadaveric hearts revealed that inflammatory molecules in the adjacent EAT were associated with the progression of MS in coronary plaques.

Fresh-Frozen Cadaveric Study

We used fresh cadaveric hearts without formaldehyde fixation, which enabled the expression of inflammatory molecules to be measured under the same conditions as in living tissues. To evaluate pericardial fat inflammation, we quantified mRNA in this tissue using the qPCR method. RNA is generally very unstable, and fixation in formalin causes nucleic acid disorders; therefore, frozen samples are considered to be more appropriate than formalin-fixed samples for quantitative assessment.[23] Formaldehyde is toxic and carcinogenic and causes mucosal irritation and respiratory damage, so the method we used prevents the adverse effects of formaldehyde on researchers. Cadavers were safely and accurately examined in the laboratory.

Inflammation in the Adjacent EAT

VEGF induces the migration and proliferation of endothelial cells, increases vascular permeability, and plays a role in tumor growth, adipose tissue expansion, age-related macular degeneration, and diabetic retinopathy.[24] CCL2 is primarily expressed by inflammatory and endothelial cells,[25] and is upregulated by pro-inflammatory stimuli and tissue injury, which are associated with atherosclerotic lesions.[26,27] A recent study reported that blood CCL2 concentrations were higher in patients with vulnerable coronary plaques.[28] McLaughlin et al reported that the expression levels of inflammatory cytokines in pericardial fat adjacent to arteriosclerotic plaques were higher than in pericardial fat adjacent to the myocardial bridge.[29] Those findings are consistent with our results. We previously reported a relationship between CAD and EAT,[10,11,30–33] and in the present study, the expression levels of *VEGF* and *CCL2* in the focal adjacent EAT were elevated in the MS (+) group, suggesting

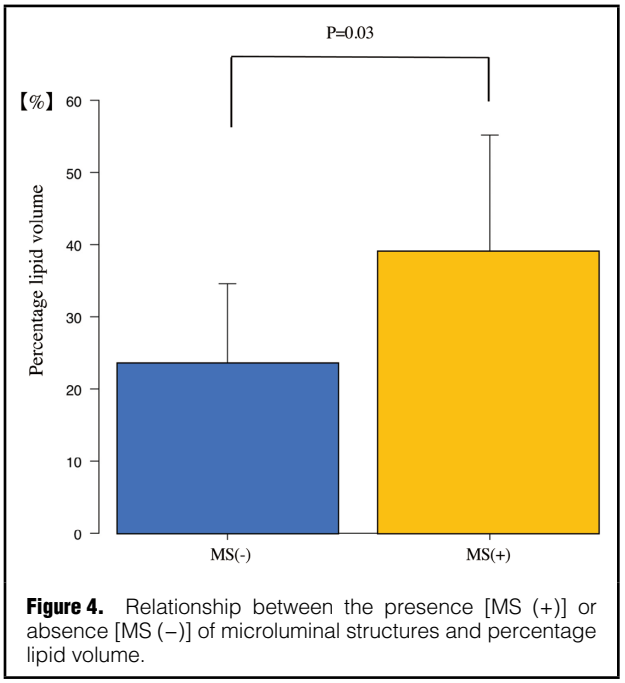

Figure 4. Relationship between the presence [MS (+)] or absence [MS (–)] of microluminal structures and percentage lipid volume.

that inflammation in the focal adjacent EAT is associated with the development of MS. Conversely, *ADIPOQ* expression levels were slightly lower in the MS (+) group. Previous studies demonstrated the cardioprotective effects of AdipoQ in vascular endothelial cells, smooth muscle cells, and cardiac myocytes.[34–36] Our results suggest similar effects of AdipoQ on the progression of MS.

MS Localization in Coronary Arteries

In the present study, the distribution of MS was slightly higher in the proximal LAD. Previous studies showed that plaques in the proximal part of the LAD had significantly higher lipid and lower fiber components than those in the distal part of the LAD.[37,38] We revealed a relationship between MS and local inflammation in EAT, suggesting a relationship between MS-mediated inflammation and plaque characteristics.

We previously reported that adventitial VV density was higher in lipid-rich lesions than in lipid-poor lesions.[33] In this study, MS also correlated with lipid-rich plaques, which taken together suggests a relationship between EAT inflammation and plaque vulnerability mediated via the VV and MS.

Intraplaque MS for the Inward Progression Theory of Vascular Inflammation

The inward progression of vascular inflammation from the adventitia towards the media and intima has been reported,[1–4,39] and furthermore, in apolipoprotein E-deficient mice the prominent VV neovascularization in the adventitia is suggested to occur prior to the initiation of coronary lesion formation.[40] In our previous[33] and present studies, we found correlations between the growth of intraplaque MS, growth of adventitial VV, and the higher expression of inflammatory molecules in adjacent EAT in fresh cadavers, supporting the important roles of the formation of intraplaque MS and adventitial VV in the pathogenesis of atherosclerosis. These results were obtained from coronary arteries without significant stenoses, and may be related to the mechanisms underlying subsequent coronary plaque progression.

Clinical Implications

The present results indicate that MS lesions (n≥1) identified by OCT are associated with inflammation in the adjacent EAT. In the clinical setting, the clinical course of MS coronary lesions needs to be closely monitored, even if they are non-stenotic. Moreover, the results obtained herein may explain one of the mechanisms underlying the clinical course and may provide beneficial information about the future progression of CAD. In addition, although pathological examinations cannot be performed during interventions, the present results suggest the utility of OCT, which is readily available in clinical settings,[41] for examining evidence of inflammation in the adjacent EAT and, thus useful information may be obtained during interventions and treatment planning.

Study Limitations

There are several limitations that need to be addressed. The sample size was small because of the limited supply of fresh cadavers. Because the repeated freezing and thawing of cadavers may affect qPCR results, we required newly thawed cadavers to assay inflammatory molecules, thereby limiting the sample size. In addition, we did not perform coronary angiography before OCT, so it was difficult to introduce the guidewire into the LAD. In some cases, we removed EAT to identify the route. Consequently, sampling sites were restricted. Furthermore, we were unable to compare the results of the pathological analysis and OCT findings with respect to MS. MS in a plaque may not be well preserved and may be lost during pathological sectioning, thereby making microscopic observations of MS difficult. Moreover, the shadow of the guidewire on an OCT image may have affected assessments of the abundance of MS. In addition, OCT images are attenuated by lipid-rich plaques, and, thus, MS may not have been detected. However, there were no unstable plaques with attenuation on OCT at any sites in the present study. Another limitation is the absence of clinical information of the cadaver other than the direct cause of death. Therefore, we were unable to exclude the possibility of anti-inflammatory and/or immunosuppressive therapies that may affect systemic inflammation. Additionally, we did not include cases of cardiovascular death, which may have precluded a more significant difference being observed.

Conclusions

Intraplaque MS observed on OCT was associated with local inflammation in the adjacent EAT and lipid-rich plaques in fresh cadaveric hearts, which suggested that local inflammation in the EAT is associated with coronary plaque vulnerability mediated via MS.

Acknowledgments

The authors thank E. Uematsu and S. Okamoto for their technical assistance with experiments, and also gratefully acknowledge the work of past and present laboratory staff.

This study was supported in part by JSPS KAKENHI Grant No. JP1589100.

Declarations of Interest / Conflicts of Interest

None.

IRB Information

Name of the Ethics Committee: Institutional Review Board of Tokushima University Hospital, Reference number: 2525-3.

References

1. Kandabashi T, Shimokawa H, Miyata K, Kunihiro I, Kawano Y, Fukata Y, et al. Inhibition of myosin phosphatase by upregulated rho-kinase plays a key role for coronary artery spasm in a porcine model with interleukin-1beta. *Circulation* 2000; **101:** 1319–1323.
2. Shimokawa H, Takeshita A. Rho-kinase is an important therapeutic target in cardiovascular medicine. *Arterioscler Thromb Vasc Biol* 2005; **25:** 1767–1775.
3. Shimokawa H, Ito A, Fukumoto Y, Kadokami T, Nakaike R, Sakata M, et al. Chronic treatment with interleukin-1 beta induces coronary intimal lesions and vasospastic responses in pigs in vivo: The role of platelet-derived growth factor. *J Clin Invest* 1996; **97:** 769–776.
4. Maiellaro K, Taylor WR. The role of the adventitia in vascular inflammation. *Cardiovasc Res* 2007; **75:** 640–648.
5. Barger AC, Beeuwkes R 3rd, Lainey LL, Silverman KJ. Hypothesis: Vasa vasorum and neovascularization of human coronary arteries: A possible role in the pathophysiology of atherosclerosis. *N Engl J Med* 1984; **310:** 175–177.
6. Shi Y, O'Brien JE, Fard A, Mannion JD, Wang D, Zalewski A. Adventitial myofibroblasts contribute to neointimal formation in injured porcine coronary arteries. *Circulation* 1996; **94:** 1655–1664.
7. Narula J, Finn AV, Demaria AN. Picking plaques that pop. *J Am Coll Cardiol* 2005; **45:** 1970–1973.
8. Moreno PR, Purushothaman KR, Zias E, Sanz J, Fuster V. Neovascularization in human atherosclerosis. *Curr Mol Med* 2006; **6:** 457–477.
9. Sacks HS, Fain JN. Human epicardial adipose tissue: A review. *Am Heart J* 2007; **153:** 907–917.
10. Tanaka K, Sata M. Roles of perivascular adipose tissue in the pathogenesis of atherosclerosis. *Front Physiol* 2018; **9:** 3.
11. Hirata Y, Tabata M, Kurobe H, Motoki T, Akaike M, Nishio C, et al. Coronary atherosclerosis is associated with macrophage polarization in epicardial adipose tissue. *J Am Coll Cardiol* 2011; **58:** 248–255.
12. Amano H, Koizumi M, Okubo R, Yabe T, Watanabe I, Saito D, et al. Comparison of coronary intimal plaques by optical coherence tomography in arteries with versus without internal running vasa vasorum. *Am J Cardiol* 2017; **119:** 1512–1517.
13. Kitabata H, Tanaka A, Kubo T, Takarada S, Kashiwagi M, Tsujioka H, et al. Relation of microchannel structure identified by optical coherence tomography to plaque vulnerability in patients with coronary artery disease. *Am J Cardiol* 2010; **105:** 1673–1678.
14. Taruya A, Tanaka A, Nishiguchi T, Matsuo Y, Ozaki Y, Kashiwagi M, et al. Vasa vasorum restructuring in human atherosclerotic plaque vulnerability: A clinical optical coherence tomography study. *J Am Coll Cardiol* 2015; **65:** 2469–2477.
15. Huang D, Swanson EA, Lin CP, Schuman JS, Stinson WG, Chang W, et al. Optical coherence tomography. *Science* 1991; **254:** 1178–1181.
16. Yamazaki H, Yamaguchi K, Soeki T, Wakatsuki T, Niki T, Taketani Y, et al. Impact of indoxyl sulfate, a uremic toxin, on non-culprit coronary plaque composition assessed on integrated backscatter intravascular ultrasound. *Circ J* 2015; **79:** 1773–1779.

17. Niki T, Wakatsuki T, Yamaguchi K, Taketani Y, Oeduka H, Kusunose K, et al. Effects of the addition of eicosapentaenoic acid to strong statin therapy on inflammatory cytokines and coronary plaque components assessed by integrated backscatter intravascular ultrasound. *Circ J* 2016; **80:** 450–460.
18. Yamaguchi K, Wakatsuki T, Soeki T, Niki T, Taketani Y, Oeduka H, et al. Effects of telmisartan on inflammatory cytokines and coronary plaque component as assessed on integrated backscatter intravascular ultrasound in hypertensive patients. *Circ J* 2014; **78:** 240–247.
19. Tanaka S, Noda T, Iwama M, Tanihata S, Kawasaki M, Nishigaki K, et al. Long-term changes in neointimal hyperplasia following implantation of bare metal stents assessed by integrated backscatter intravascular ultrasound. *Heart Vessels* 2013; **28:** 415–423.
20. Kanda Y. Investigation of the freely available easy-to-use software 'EZR' for medical statistics. *Bone Marrow Transplant* 2013; **48:** 452–458.
21. Patel VB, Shah S, Verma S, Oudit GY. Epicardial adipose tissue as a metabolic transducer: Role in heart failure and coronary artery disease. *Heart Fail Rev* 2017; **22:** 889–902.
22. Gaborit B, Sengenes C, Ancel P, Jacquier A, Dutour A. Role of epicardial adipose tissue in health and disease: A matter of fat? *Compr Physiol* 2017; **7:** 1051–1082.
23. Hatanaka Y, Kuwata T, Morii E, Kanai Y, Ichikawa H, Kubo T, et al. The Japanese Society of Pathology Practical Guidelines on the handling of pathological tissue samples for cancer genomic medicine. *Pathol Int* 2021; **71:** 725–740.
24. Greenberg DA, Jin K. Vascular endothelial growth factors (VEGFs) and stroke. *Cell Mol Life Sci* 2013; **70:** 1753–1761.
25. Ferrara N, Davis-Smyth T. The biology of vascular endothelial growth factor. *Endocr Rev* 1997; **18:** 4–25.
26. Deshmane SL, KremLev S, Amini S, Sawaya BE. Monocyte chemoattractant protein-1 (MCP-1): An overview. *J Interferon Cytokine Res* 2009; **29:** 313–326.
27. Cahill PA, Redmond EM. Vascular endothelium: Gatekeeper of vessel health. *Atherosclerosis* 2016; **248:** 97–109.
28. Ragino YI, Striukova EV, Murashov IS, Polonskaya YV, Volkov AM, Kurguzov AV, et al. Association of some hemostasis and endothelial dysfunction factors with probability of presence of vulnerable atherosclerotic plaques in patients with coronary atherosclerosis. *BMC Res Notes* 2019; **12:** 336.
29. McLaughlin T, Schnittger I, Nagy A, Zanley E, Xu Y, Song Y, et al. Relationship between coronary atheroma, epicardial adipose tissue inflammation, and adipocyte differentiation across the human myocardial bridge. *J Am Heart Assoc* 2021; **10:** e021003.
30. Maimaituxun G, Shimabukuro M, Fukuda D, Yagi S, Hirata Y, Iwase T, et al. Local thickness of epicardial adipose tissue surrounding the left anterior descending artery is a simple predictor of coronary artery disease: New prediction model in combination with Framingham Risk Score. *Circ J* 2018; **82:** 1369–1378.
31. Dagvasumberel M, Shimabukuro M, Nishiuchi T, Ueno J, Takao S, Fukuda D, et al. Gender disparities in the association between epicardial adipose tissue volume and coronary atherosclerosis: A 3-dimensional cardiac computed tomography imaging study in Japanese subjects. *Cardiovasc Diabetol* 2012; **11:** 106.
32. Hirata Y, Yamada H, Kusunose K, Iwase T, Nishio S, Hayashi S, et al. Clinical Utility of measuring epicardial adipose tissue thickness with echocardiography using a high-frequency linear probe in patients with coronary artery disease. *J Am Soc Echocardiogr* 2015; **28:** 1240–1246.e1241.
33. Ito H, Wakatsuki T, Yamaguchi K, Fukuda D, Kawabata Y, Matsuura T, et al. Atherosclerotic coronary plaque is associated with adventitial vasa vasorum and local inflammation in adjacent epicardial adipose tissue in fresh cadavers. *Circ J* 2020; **84:** 769–775.
34. Matsuda M, Shimomura I, Sata M, Arita Y, Nishida M, Maeda N, et al. Role of adiponectin in preventing vascular stenosis: The missing link of adipo-vascular axis. *J Biol Chem* 2002; **277:** 37487–37491.
35. Kobayashi H, Ouchi N, Kihara S, Walsh K, Kumada M, Abe Y, et al. Selective suppression of endothelial cell apoptosis by the high molecular weight form of adiponectin. *Circ Res* 2004; **94:** e27–e31.
36. Ouchi N, Kobayashi H, Kihara S, Kumada M, Sato K, Inoue T, et al. Adiponectin stimulates angiogenesis by promoting cross-talk between AMP-activated protein kinase and Akt signaling in endothelial cells. *J Biol Chem* 2004; **279:** 1304–1309.
37. Komura N, Hibi K, Kusama I, Otsuka F, Mitsuhashi T, Endo M, et al. Plaque location in the left anterior descending coronary artery and tissue characteristics in angina pectoris: An integrated backscatter intravascular ultrasound study. *Circ J* 2010; **74:** 142–147.
38. Slager CJ, Wentzel JJ, Gijsen FJ, Schuurbiers JC, van der Wal AC, van der Steen AF, et al. The role of shear stress in the generation of rupture-prone vulnerable plaques. *Nat Clin Pract Cardiovasc Med* 2005; **2:** 401–407.
39. Shimokawa H. 2014 Williams Harvey Lecture: Importance of coronary vasomotion abnormalities: From bench to bedside. *Eur Heart J* 2014; **35:** 3180–3193.
40. Tanaka K, Nagata D, Hirata Y, Tabata Y, Nagai R, Sata M. Augmented angiogenesis in adventitia promotes growth of atherosclerotic plaque in apolipoprotein E-deficient mice. *Atherosclerosis* 2011; **215:** 366–373.
41. Kurogi K, Ishii M, Yamamoto N, Yamanaga K, Tsujita K. Optical coherence tomography-guided percutaneous coronary intervention: A review of current clinical applications. *Cardiovasc Interv Ther* 2021; **36:** 169–177.